doi: 10.82124/CEAS-GNC-2026-087 CEAS-GNC-2026-087

EuroGNC Navigation Guidance Control CEAS Madrid, Spain May 5th-7th uc3m Universidad Carlos III de Madrid AIAA 2026

A design approach for the systematic synthesis of rotorcraft control laws

Pietro Bruschi PhD Student, Politecnico di Milano, Milan, Italy. pietro.bruschi@polimi.it

Marco Lovera Full Professor, Politecnico di Milano, Milan, Italy. marco.lovera@polimi.it

ABSTRACT

This paper presents an approach to the systematic synthesis of fixed-structure control laws for rotorcraft. The proposed approach enables the design of attitude controllers capable of stabilizing helicopter dynamics across multiple flight conditions, from hover to high-speed flight. The approach leverages multi-objective structured H_∞ synthesis on a model representative of a helicopter's attitude dynamics. Both hard and soft performance requirements are considered, taken from standard design literature, including disk margins and constraints on the sensitivity function to manage inter-axis coupling. An illustrative case demonstrates the tool's capability to achieve satisfactory closed-loop performance, validating its potential for rotorcraft control law design and certification support.

Keywords: Flight Control Laws, H_∞ synthesis, Rotorcraft control

Nomenclature

0_N	=	zeros matrix of dimension N
α, β	=	low- and high-frequency gains [-]
γ_H	=	best achieved hard constraint values [-]
γ_S	=	best achieved soft constraint values [-]
δ_{col}	=	normalized main rotor collective command [-]
δ_{lat}	=	normalized cyclic command (lateral) [-]
δ_{lon}	=	normalized cyclic command (longitudinal) [-]
δ_{ped}	=	normalized tail rotor collective command [-]
ξ	=	vector of tunable parameters
φ, θ, ψ	=	roll, pitch, and yaw angles [deg]
A, B, C, D	=	state-space matrices of the plant model
f	=	frequency [Hz]
I_N	=	identity matrix of dimension N
n	=	model order
n_ξ	=	number of tunable parameters
n_u	=	number of inputs
n_y	=	number of outputs
p, q, r	=	roll, pitch, and yaw rate [deg/s]
s	=	Laplace variable [-]
u, v, w	=	body-fixed translational velocities [ft/s]

1 Introduction

Helicopters represent exceptionally versatile aerial platforms. Their unique capabilities make them indispensable for a wide range of applications, encompassing both civil and military missions. However, this versatility comes at the cost of significant dynamical complexity. Helicopters exhibit strong coupling effects, pronounced nonlinearities, and, in most cases, significant open-loop instability, which makes control design a demanding task. Additionally, uncertainties arising from unmodeled dynamics, parameter variations, sensor noise, and external disturbances can significantly degrade flight performance and compromise safety. These characteristics make the development of robust and reliable flight control laws a central challenge in rotorcraft engineering. Specifically, meeting all the standard requirements set by certification bodies can be challenging, often necessitating trade-offs.

Consequently, the design of flight control laws remains one of the most challenging and active areas of research in modern rotorcraft technology. Traditional control strategies often struggle to maintain satisfactory performance throughout the entire flight envelope due to parameter variations and unmodeled dynamics. Therefore, it is essential to develop *structured control laws*, capable of accounting for a sufficiently complex helicopter's model, while ensuring stability and performance. In the past, the CONDUIT tool [1] has proven to be effective in designing helicopters' flight control laws. Indeed, it supports the design and the analysis of advanced aerospace control systems, explicitly accounting for identified uncertainties, and integrating nonlinear analysis [2].

Specifically, structured H_∞ synthesis has emerged as an effective approach for designing controllers that achieve a trade-off between robustness and performance by formulating the control problem as a constrained optimization task [3] [4]. This method, especially in the multivariable case [5], fits well with rotorcraft controllers, since it preserves the predefined controller structures, such as low-order, gain-scheduled architectures, thus facilitating physical interpretability and implementation, and aligns more closely with industrial certification standards. Indeed, it has been applied to the design of helicopter controllers [6] [7] as well as to other similar technologies [8]. The *multi-model, multi-objective* framework further enhances this approach [9], by allowing simultaneous optimization of control performance across multiple linearized models that represent, *e.g.*, different flight conditions or operating regimes [10]. This is particularly relevant in the rotorcraft context, since they exhibit strongly coupled and parameter-varying dynamics across their flight envelope.

Rotorcraft handling qualities are specified in the ADS-33E-PRF US Army standard [11]. Several studies have shown how such requirements may be translated into control-oriented constraints and incorporated into systematic synthesis procedures [6] [12]. In particular, recent structured H_∞-based methodologies have demonstrated the potential of combining handling-quality requirements with fixed-structure robust synthesis. However, existing approaches still present important limitations. Some methods rely on decentralized or axis-by-axis tuning philosophies, which may not fully capture the strongly coupled nature of helicopter attitude dynamics. For instance, recent work has addressed the longitudinal channel through a decentralized structured H_∞ framework, showing promising results but remaining restricted to a single-axis problem rather than a fully coupled Multiple Input Multiple Output (MIMO) attitude-control architecture [13].

In this work, a multi-objective framework for the synthesis of helicopters' flight control laws is presented. Specifically, a command augmentation system is considered, with an attitude command-attitude hold (ACAH) flight control system. Unlike recent works [10], the proposed approach presents a hierarchical architecture with nested loops, integrated with a structured multi-objective H_∞ synthesis framework for a fully coupled MIMO rotorcraft problem. More precisely, unlike approaches limited to one axis or based on decentralized formulations, the proposed architecture is designed to account explicitly for inter-axis couplings during synthesis, so that all attitude channels are addressed simultaneously within the same optimization problem.

The main contribution of this paper is therefore not only a synthesis tool refinement, but a structured design methodology for flight-control-law engineers that enables the straightforward synthesis of fully coupled MIMO controllers for rotorcraft attitude control, while preserving an implementable hierarchical architecture. The method is formulated in a way that is largely agnostic to the specific rotorcraft configuration, provided that sufficiently complete models are available. In addition, it leaves to the designer a clear and physically meaningful tuning choice, namely the target attitude bandwidth of the closed-loop system, while automatically handling the multi-objective robust synthesis problem and the associated coupling trade-offs. This makes the approach attractive both from a design perspective and from the viewpoint of practical implementation and certification-oriented development.

The remainder of the manuscript is organized as follows. In Section II the formulation of the problem is presented: the various blocks composing the loop are described, and the requirements are listed. Section III illustrates the set up of the optimization process, including the weight functions selected for the fulfillment of the requirements. In Section VI, an example on the application of the method to the data of the Bo-105 helicopter, at 120 kts and 3000 ft are presented, demonstrating the efficiency of such a tool, producing controllers with satisfactory performance, especially in terms of inter-axis couplings. Finally, Section V draws the conclusions and lists some possible improvements and future works.

2 Problem Formulation

In this section, the problem formulation is presented in detail. First, the overall system architecture and its constituent blocks are described, providing an overview of the model structure. Each subsystem is characterized in terms of its function and interaction with the others, forming the foundation for subsequent analysis and controller design. Following the system description, the performance and handling requirements that the closed-loop system must satisfy are outlined. These requirements are established in accordance with the ADS-33E-PRF handling qualities specification, which defines the performance and control criteria for rotorcraft flight dynamics. Specifically, the requirements considered in this work encompass disturbance rejection, inter-axis couplings, and stability margins.

2.1 Design System Architecture

The proposed approach is primarily designed for application on helicopters and other rotorcraft systems. However, its structure is intentionally kept general and flexible. The model requires, as its plant component $G(s)$, one or more *linear time-invariant* (LTI) systems, which represent the dynamic behavior of the physical system under consideration. The control component is defined by a general *linear controller* $K(s)$, allowing for a wide range of control strategies to be implemented and analyzed. In the following sections, the selected system architecture adopted for the model under investigation is presented, detailing the specific configuration, interaction among components, and rationale behind the chosen control design.

Plant Model

The model under study is the one detailed in [14], and it is a model representative of the attitude dynamics of the Bo-105 helicopter. The plant $G(s) \in \mathbb{R}(s)^{n_y \times n_u}$, where $\mathbb{R}(s)$ indicates the set of rational proper transfer functions, may be written in state-space form:

$$G(s) : \begin{cases} \dot{x} = Ax + Bu \\ y = Cx + Du \end{cases} . \tag{1}$$

The model receives $n_u = 4$ inputs and produces $n_y = 9$ outputs, encompassing $n = 53$ states, subdividing in the following way the vector $x \in \mathbb{R}^n$:

- The first nine states correspond to the rigid-body dynamics of the rotorcraft. These include the translational velocities, angular rates, and Euler angles, which collectively describe the vehicle's overall motion and orientation in space.
- The subsequent eight states capture the dynamics associated with the first elastic (flapping) mode of the rotor blades, representing the primary structural flexibility effects that influence the rotor's response.
- Similarly, an additional eight states are used to model the second elastic mode, and this pattern continues up to the fifth mode, thereby accounting for the higher-order elastic deformations of the blades. Including multiple modes ensures an accurate representation of the blade dynamics across a wide frequency range.
- Furthermore, three states are dedicated to modeling the dynamic inflow of the main rotor, which characterizes the unsteady aerodynamic effects and induced velocity distribution in the rotor's wake.
- Finally, one additional state represents the dynamic inflow of the tail rotor, capturing the corresponding unsteady aerodynamic behavior that affects yaw control and overall rotorcraft stability.

The model retains in the output $y \in \mathbb{R}^{n_y}$ only the translational velocities in body axes, expressed in ft/s, the angular rates, expressed in deg/s, and the Euler angles, expressed in deg:

$$y = [y_{\text{vel}}^\top \; y_{\text{rate}}^\top \; y_{\text{ang}}^\top]^\top,$$

$$\text{with} \quad y_{\text{vel}} = [u \; v \; w]^\top \in \mathbb{R}^3, \quad y_{\text{rate}} = [p \; q \; r]^\top \in \mathbb{R}^3, \quad \text{and} \quad y_{\text{ang}} = [\varphi \; \theta \; \psi]^\top \in \mathbb{R}^3.$$

The input vector $u \in \mathbb{R}^{n_u}$, instead, collects the normalized commands of the helicopter, namely the main rotor collective, the cyclic lateral and longitudinal, and the tail rotor collective, expressed as the amount of throttle:

$$u = [\delta_{\text{col}} \; \delta_{\text{lat}} \; \delta_{\text{lon}} \; \delta_{\text{ped}}]^\top.$$

The model is available for several different flight conditions, ranging from hover to 160 kts speed. The model at 120 kts is selected as an example for our study. In principle, the controllers obtained for every different flight condition may be merged through an appropriate *gain-scheduling* technique, we will not expand on this topic since already covered by existing works.

The open-loop plant is typically replaced with a scaled version $G^{\text{sc}}(s) \in \mathbb{R}^{n_y \times n_u}$, given by $G^{\text{sc}}(s) = P_y^{-1} G(s) P_u$ [15]. Here, $P_y \in \mathbb{R}^{n_y \times n_y}$ and $P_u \in \mathbb{R}^{n_u \times n_u}$ are constant diagonal matrices of appropriate dimensions, and their inverses scale the inputs and outputs of $G(s)$ respectively. In particular, P_u is selected so that the maximum allowed control input is normalized to 1:

$$P_u = I_4.$$

P_y normalizes the output to 1, and its precise value is determined through an iterative procedure:

$$P_y = \begin{bmatrix} 10I_3 & 0_3 & 0_3 \\ 0_3 & 1I_3 & 0_3 \\ 0_3 & 0_3 & 360I_3 \end{bmatrix}.$$

The model is placed inside a control loop. Once again, the procedure outlined is general and works, in principle, with any linear controller. However, we will present the case of a rotorcraft control application, where a hierarchical control structure is employed, thus designing two separate controllers aiming at regulating the attitude and the rate loop, respectively.

Controller Architecture

The structure of the system designed is illustrated in Figure 1[1].

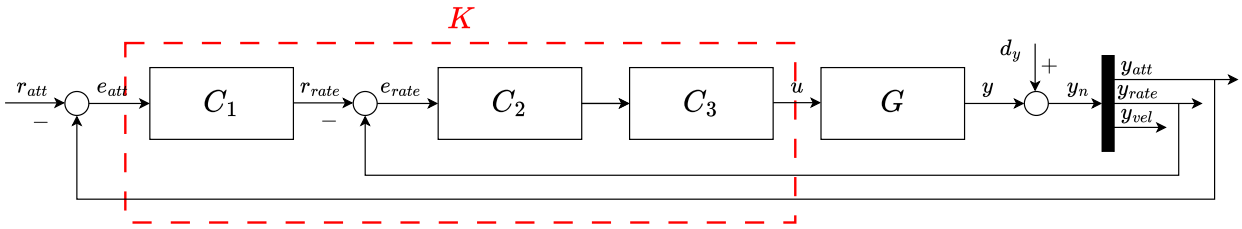

Fig. 1 Control Architecture Scheme.

The various blocks present in the figure are now briefly described. The inputs of the closed-loop system are an attitude reference signal r_{att}, commanded by the pilot and acting at the upper level, and a disturbance input d_y, that accounts for uncertainties arising from sensors and unmodeled dynamics, injected into the output y. Thus, we can define the noisy measurement and the control error as follows:

$$y_{\text{n}} = y + d_y \tag{2}$$
$$e_{\text{att}} = r_{\text{att}} - y_{\text{att}} \tag{3}$$
$$e_{\text{rate}} = r_{\text{rate}} - y_{\text{rate}}, \tag{4}$$

having defined reference vectors r_{att}, $r_{\text{rate}} \in \mathbb{R}^3$ and the noise vector $d_y \in \mathbb{R}^9$ as follows:

$$r_{\text{att}} = [r_\varphi \; r_\theta \; r_\psi]^\top, \quad r_{\text{rate}} = [r_p \; r_q \; r_r]^\top, \quad \text{and} \quad d_y = [d_u \; d_v \; d_w \; d_p \; d_q \; d_r \; d_\varphi \; d_\theta \; d_\psi]^\top. \tag{5}$$

The controller block $K(s) \in \mathbb{R}^{4\times3}$ encompasses the controllers $C_1(s)$, $C_2(s)$, and $C_3(s)$.

The block $C_1(s) \in \mathbb{R}(s)^{3\times3}$ acts on the attitude error and produce the reference for the rate loop, that feeds $C_2(s) \in \mathbb{R}(s)^{3\times3}$, which acts on the rate error. Both controllers have the same structure, with a proportional integral (PI) action:

$$C_i(s) = K_{Pi} + K_{Ii}\frac{1}{s}, \quad i = 1, 2; \tag{6}$$

having defined the matrices $K_{Pi} \in \mathbb{R}^{3\times3}$ and $K_{Ii} \in \mathbb{R}^{3\times3}$ as follows:

$$K_{Pi} = \begin{bmatrix} K^i_{Pp} & 0 & 0 \\ 0 & K^i_{Pq} & 0 \\ 0 & 0 & K^i_{Pr} \end{bmatrix}, \quad K_{Ii} = \begin{bmatrix} K^i_{Ip} & 0 & 0 \\ 0 & K^i_{Iq} & 0 \\ 0 & 0 & K^i_{Ir} \end{bmatrix}$$

with the non-zero elements of the matrices used as tunable parameters in the optimization process.

Finally, the block $C_3(s) \in \mathbb{R}(s)^{4\times3}$ maps the control actions on the corresponding input channels, with an additional sequence of poles and zeros, to be treated as tunable parameters as well:

$$C_3(s) = \begin{bmatrix} 0 & 0 & 0 \\ C_{3\varphi}(s) & 0 & 0 \\ 0 & C_{3\theta}(s) & 0 \\ 0 & 0 & C_{3\psi}(s) \end{bmatrix}. \tag{7}$$

[1]In the figures the dependence on the Laplace variable s has been omitted for brevity.

More precisely, each of the non-zero elements of $C_3(s)$ has the following form:

$$C_{3j}(s) = \frac{(1 + z_1 s) \cdots (1 + z_{n_{zj}})}{(1 + p_1 s) \cdots (1 + p_{n_{pj}})} \quad j = \varphi, \theta, \psi. \tag{8}$$

In this work, the number of poles and zeros has been considered to be the same, *i.e.*, $n_{zj} = n_{pj}$. Furthermore, this number has been fixed for all axes: $n_{z\varphi} = n_{z\theta} = n_{z\psi} = 3$.
Equation (7) shows that no command is assigned to the main rotor collective, as reflected in the first row, since the present study is restricted to the attitude control problem.

2.2 Design System Requirements

Once the closed-loop model has been constructed, the introduced controllers have to be tuned according to a set of requirements imposed by the designer. Such requirements may be taken either from standards, such as the ADS-33 [11], or found in the proposed literature. In the present work, stability margins and disturbance rejection bandwidth [16], as well as stability, are considered. Furthermore, both soft and hard requirements are considered: the latter are mandatory conditions for the optimizer that must be met, while the former are desirable preferences that are not strictly necessary. The soft requirements are given by the disk margins, which ensures that the closed-loop system retains satisfactory stability margins under plant perturbations. The hard requirement is placed on the sensitivity function $S(s)$, whose frequency response is shaped to achieve the desired closed-loop performance, particularly in terms of disturbance attenuation, reference tracking, and steady-state accuracy.

Disk-based Margins

The disk-based margins [17] can be used to set a tuning goal. They are selected since, according to recent works [10], they are more reliable with respect to their classical counterpart (gain margin and phase margin) because they consider simultaneously variations of both gain and phase.

The margins adopted in this work are taken from the available literature, and are reported hereafter, in Table 1:

Table 1 Gain and phase margins imposed.

Frequency Range	Service Envelope Margins
$f_L \leq f \leq f_U$	GM = ±4.5 dB PM = ±30°

Given the open-loop transfer function $L(s) = K(s)G(s)$, game and phase variations may be modeled as a complex perturbation on $L(s)$, that lies inside a disk in the complex plane, shown in Figure 2. Such disk is parametrized by a real scalar α_D, retrieved from the most stringent requirement between the minimum gain margin GM and the minimum phase margin PM. For a complete description of disk-based margins, readers are referred to [17].

The chosen margins are valid for a generic service envelope. Moreover, a frequency range of interest has been selected:

$$f_L = 0.01 \text{ Hz}, \quad f_U = 2 \text{ Hz}.$$

This frequency range is selected based on piloted handling qualities criteria. At higher frequencies, the dynamics become either uncontrollable or dominated by noise. Additionally, strong couplings with the main rotor harmonics render it impractical to analyze or design control laws in that region.

Disk-based margins are imposed as a soft requirement on the attitude loop.

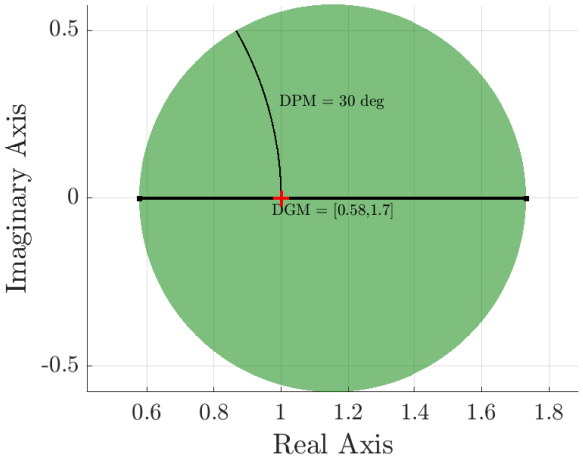

Fig. 2 Disk Margins.

Sensitivity Function

The only hard requirement is imposed on the sensitivity function $S(s) \in \mathbb{R}(s)^{3\times3}$, defined as the transfer function from the reference vector to the error vector:

$$S(s) = (I_3 + L(s))^{-1}.$$

Such a requirement allows to shape the sensitivity function of the closed-loop system, thus acting on the performance and on the disturbance rejection response [18]. Figure 3 highlights the forbidden regions of the sensitivity function for direct response terms (left) and inter-axis coupling terms (right). The choice of the specific weights for the controller synthesis is discussed in Section 3.

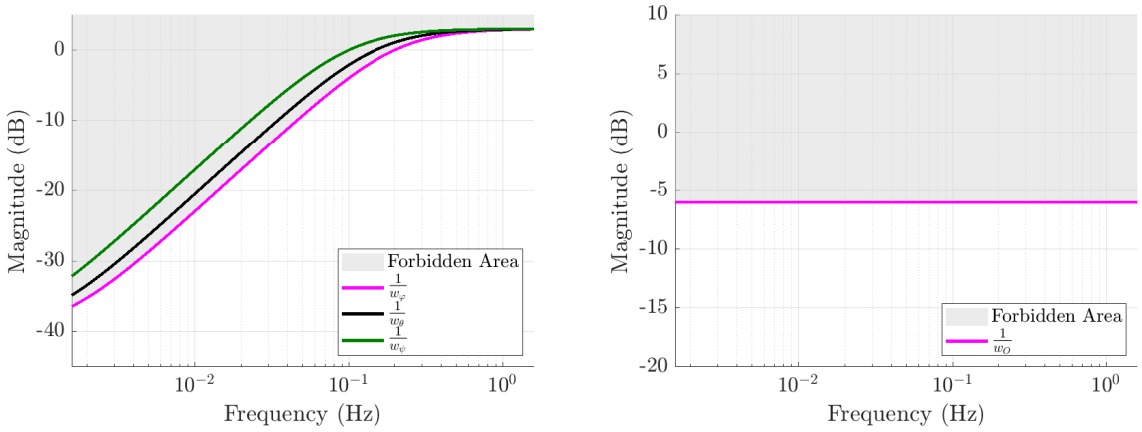

(a) **(b)**

Fig. 3 Allowed and forbidden region for $S(s)$ in direct responses (a), and inter-axis couplings (b).

3 Synthesis Framework

In this section, the set-up of the optimization framework is introduced. First, the weights used to impose the requirements are presented, and then the mathematics behind the optimization process is illustrated.

3.1 Multi-Objective Weights

While disk-based margins may be directly passed to the optimizer, the sensitivity function requirement is imposed through the definition of a weight function. Such a weight is chosen as a first-order filter for direct response terms:

$$w_i(s) = \frac{\frac{s}{\beta} + \omega_{ci}}{s + \alpha\omega_{ci}}, \quad \text{with} \quad i = 1, 2, 3, \tag{9}$$

where $w_i(s)$ represents the i-th diagonal entry of the matrix $W(s) \in \mathbb{R}(s)^{3\times3}$ and ω_{ci} the corresponding element of the cross-over frequency vector: $\omega_c = [\omega_\varphi \ \omega_\theta \ \omega_\psi]^\top$. The low-frequency gain α is chosen such that $w_i(0) = \frac{1}{\alpha}$, while the high-frequency gain β is defined such that $w_i(\infty) = \frac{1}{\beta}$. The cross-over frequencies are the only parameters that the designer is asked to tune, according to the desired velocity of the response. A constant weight is set for inter-axis coupling terms, namely the off-diagonal terms of $S(s)$:

$$w_O = 10^{\frac{6}{20}}, \tag{10}$$

that translates in having the inter-axis coupling terms magnitude always below -6 dB in the frequency range of interest.

Given the vector of tunable parameters $\xi \in \mathbb{R}^{n_\xi}$, the soft requirements are collected in a vector $J_{n_S}(\xi)$, while the hard requirements are collected in a vector $H_{n_H}(\xi)$ such that:

$$H_{n_H}(\xi) = ||W_S(s)S(s,\xi)||_\infty. \tag{11}$$

In Figure 4, the closed-loop scheme, updated with the weight function, is reported.

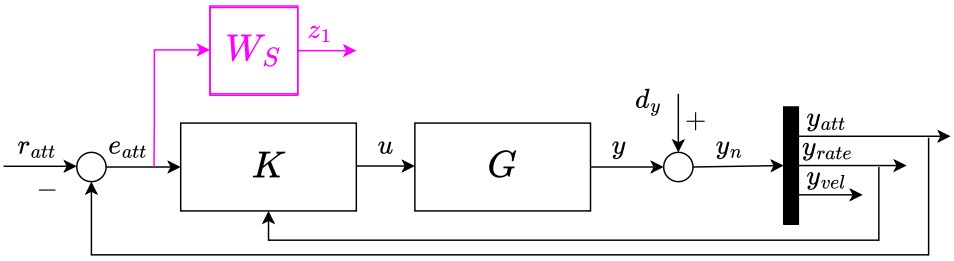

Fig. 4 Control Architecture Scheme with Sensitivity weight.

3.2 Synthesis Process

As remarked in the Introduction, the synthesis process follows a multi-objective H_∞ approach, with the model coming from [14] and the objectives specified in the previous subsection.

The synthesis approach may be formalized as follows. Let $K(s,\xi)$ be a structured LTI controller represented in the Laplace domain, dependent on a vector of tunable parameters ξ. Given n_H hard objectives, collected in a vector $H_{n_H}(\xi)$, and n_S soft requirements, collected in a vector $J_{n_S}(\xi)$, the optimization process can be cast as finding the parameters vector ξ that solves

$$\min_\theta \max_{j=1,\dots,n_S} J_j(\xi) \quad \text{subject to} \quad \max_{k=1,\dots,n_H} H_k(\xi) \leq 1$$

while guaranteeing that the closed-loop system is stable.

The synthesis tool returns the tuned parameters — thus, the found controllers — and the best value obtained for the two cost functions γ_S, γ_H. They can be translated to worst-case tuning goal for each objective: a value smaller than 1 implies that the goal is satisfied, values close to 1 are still acceptable.

4 Numerical Results

This section illustrates the simulation results obtained for the data of the Bo-105 helicopter, flying at 3000 ft altitude with a speed of 120 kts.

The cross-over frequencies selected for the synthesis are:

- Roll axis: $\omega_\varphi = 0.20$ Hz.
- Pitch axis: $\omega_\theta = 0.15$ Hz.
- Yaw axis: $\omega_\psi = 0.10$ Hz.

The synthesis is performed and the results are obtained. The weight function has been divided in two components, in order to study separately the behaviour of direct responses ($W_S(s)$) and inter-axis couplings ($W_O(s)$), such that:

$$W(s) = W_S(s) + W_O(s). \tag{12}$$

The two matrices are, respectively, the diagonal and the off-diagonal parts of the matrix $W(s)$.

Table 2 Achieved constraints values .

	γ_H	γ_S
Achieved Value	$W_S(s)$: 1.2087 $W_O(s)$: 1.1647	DM: 0.7605

Table 2 shows the obtained results, in terms of best achieved values, for both hard and soft constraints (DM). The latter are always satisfied, according to the obtained γ_S, while the former are satisfied for the majority of the frequency range of interest.

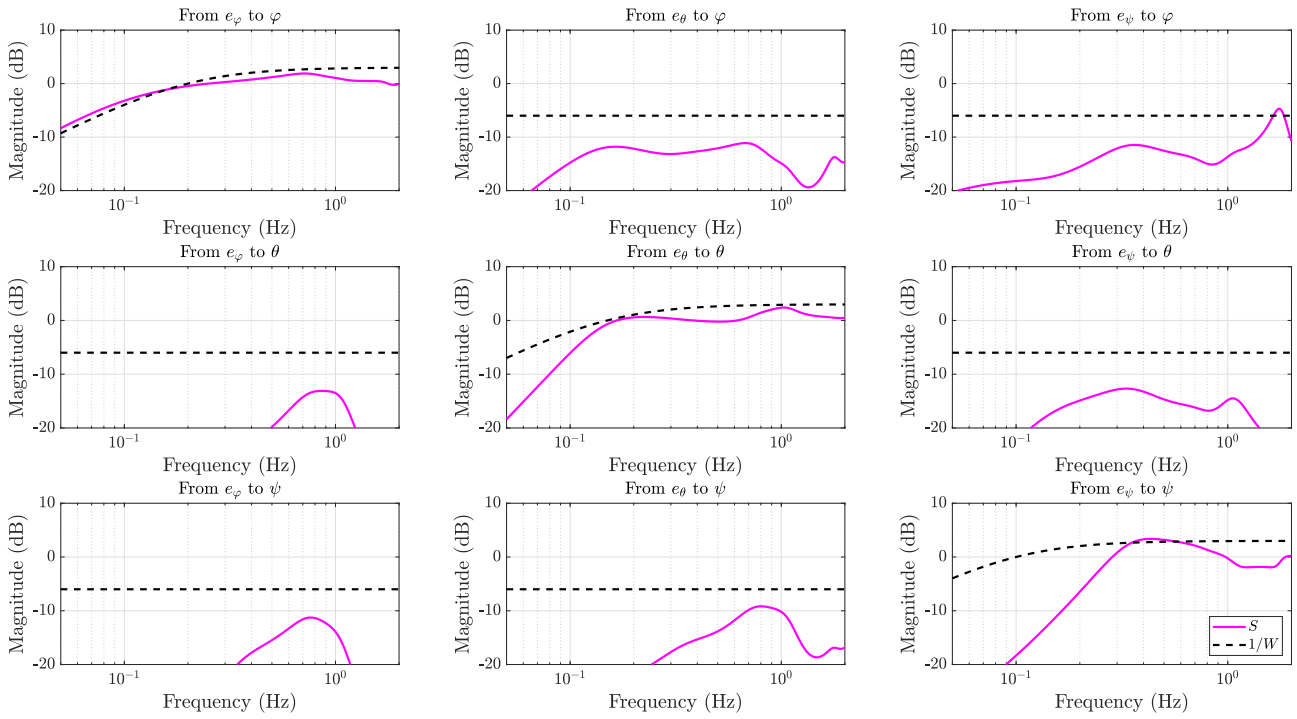

Fig. 5 Sensitivity function plot.

Figure 5 displays the sensitivity function for the outer loop, compared with the imposed weight. The results show that the found controller led to satisfactory performance, both in terms of sensitivity function of the direct responses, but especially regarding inter-axis coupling terms, which are kept limited.

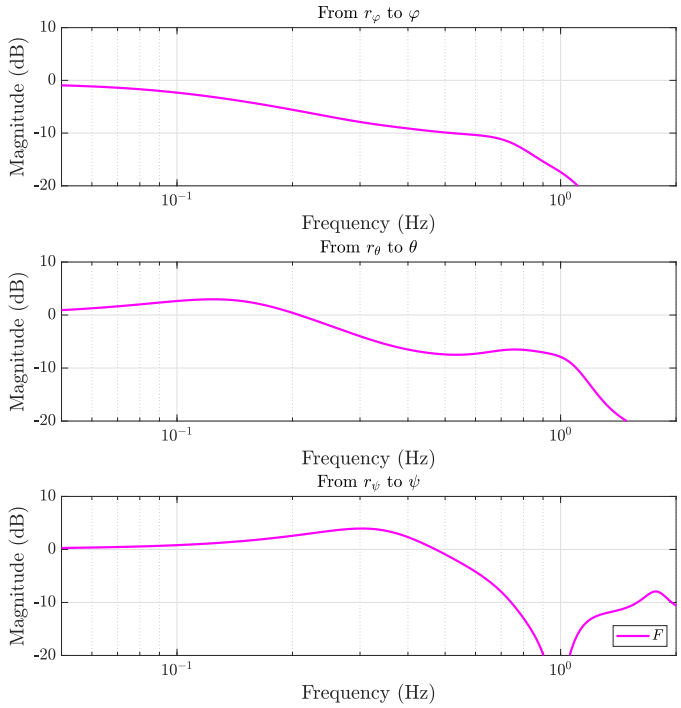

Fig. 6 Complementary Sensitivity Function Plot.

In Figure 6 the complementary sensitivity function $F(s) \in \mathbb{R}(s)^{3\times3}$ is reported. Results demonstrate, once again, that acceptable attitude bandwidths are obtained. For the complementary sensitivity function only the diagonal terms are reported, to avoid repetitions.

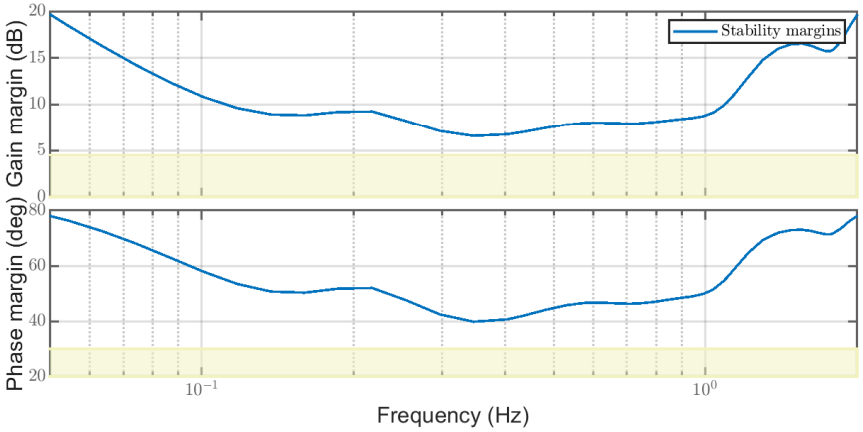

Fig. 7 Stability Margins Plots.

Finally, Figure 7 shows the stability margins of the system as a function of the frequency. Notably, in the frequency range of interest, both gain and phase margins are always above the imposed requirement (defined by the yellow area □).

5 Conclusions

The approach proposed in this work has proven effective in generating structured controllers, achieving satisfactory performance levels. Notably, the controllers synthesized using this framework exhibit efficient management of inter-axis coupling effects, enhancing overall system stability and responsiveness.

The methodology is fully general and can be applied to any type of linear controller. This flexibility allows designers to tailor the control loops according to desired specification, such as selecting the appropriate attitude bandwidth for each loop.

Future research will focus on extending the framework to handle systems with uncertainties, enabling robust control analysis and synthesis. Additionally, the authors plan to explore the incorporation of concentrated nonlinearities into the models to assess their impact on system behavior and to develop strategies for mitigating potential adverse effects.

Declaration of Use of Artificial Intelligence

Artificial Intelligence was used for proofreading and translation.

References

[1] Mark Tischler, Jason Colbourne, Mark Morel, Daniel Biezad, William Levine, and Veronica Moldoveanu. CONDUIT: A New Multidisciplinary Integration Environment for Flight Control Development. 1997. doi: 10.2514/6.1997-3773.

[2] Mark Tischler, James Lee, and Jason Colbourne. Comparison of flight control system design methods using the CONDUIT design tool. *Journal of Guidance, Control, and Dynamics*, 25(3):482–493, 2002. doi: 10.2514/2.4908.

[3] Pierre Apkarian and Dominikus Noll. Nonsmooth H_∞ Synthesis. *IEEE Transactions on Automatic Control*, 51(1):71–86, 2006. doi: 10.1109/TAC.2005.860290.

[4] Pascal Gahinet and Pierre Apkarian. Structured H_∞ synthesis in MATLAB. *IFAC Proceedings Volumes*, 44(1):1435–1440, 2011. 18th IFAC World Congress. doi: 10.3182/20110828-6-IT-1002.00708.

[5] Ian Postlethwaite. *Multivariable Feedback Control: Analysis and Design*. John Wiley & Sons, Inc., USA, 1996. ISBN: 0471943304.

[6] Jean-Marc Biannic, Armin Taghizad, Lucie Dujols, and Gabriele Perozzi. A multi-objective H_∞ design framework for helicopter PID control tuning with handling qualities requirements. 2017. doi: 10.13009/EUCASS2017-51.

[7] Matthew C. Turner, Daniel J. Walker, and Adrian G. Alford. Design and ground-based simulation of an H_∞ limited authority flight control system for the Westland Lynx Helicopter. *Aerospace Science and Technology*, 5(3):221–234, 2001. doi: 10.1016/S1270-9638(01)01093-8.

[8] Simone Panza, Marco Lovera, Masayuki Sato, and Koji Muraoka. Structured -synthesis of robust attitude control laws for quad-tilt-wing unmanned aerial vehicle. *Journal of Guidance, Control, and Dynamics*, 43(12):2258–2274, 2020. doi: 10.2514/1.G005080.

[9] Pierre Apkarian, Pascal Gahinet, and Craig Buhr. Multi-model, multi-objective tuning of fixed-structure controllers. In *2014 European Control Conference (ECC)*, pages 856–861, 2014. doi: 10.1109/ECC.2014.6862200.

[10] Patrick Authié. A multi-model and multi-objective approach to the design of helicopter flight control laws. *CEAS Aeronautical Journal*, 15(3):529–543, 2024. doi: 10.2514/2.4908.

[11] U.S. Army Aviation and Missile Command. ADS-33E-PRF: Handling Qualities Requirements for Military Rotorcraft. Technical report, 2000.

[12] J.C. Antonioli, A. Taghizad, T. Rakotomamonjy, and M. Ouladsine. Towards the development of a methodology for designing helicopter flight control laws by integrating handling qualities requirements from the first stage of tuning. In *40th European Rotorcraft Forum (ERF 2014)*, Southampton, United Kingdom, Sept. 2014. `https://hal.science/hal-01094364`.

[13] Tommaso Capra, Spilios Theodoulis, and Marilena Pavel. Multi-objective design of a decentralized structured H_∞-based controller for longitudinal helicopter flight dynamics. In *AIAA SCITECH 2025 Forum*. doi: 10.2514/6.2025-2244.

[14] Colin Theodore and Roberto Celi. Helicopter Flight Dynamic Simulation with Refined Aerodynamics and Flexible Blade Modeling. *Journal of Aircraft*, 39:577–586, 2002. doi: 10.2514/2.2995.

[15] Pietro Bruschi, Davide Invernizzi, Mauro Massari, and Marco Lovera. Coordinated manipulator/spacecraft control with systematic gain tuning for space robot operations. *Journal of Guidance, Control, and Dynamics*, 49(2):561–576, 2026. doi: 10.2514/1.G008811.

[16] Mark Tischler, Christina Ivler, Hossein Mansur, Kenny Cheung, Tom Berger, and Marcos Berrios. Handling-Qualities Optimization and Trade-offs in Rotorcraft Flight Control Design. 2008.

[17] Peter Seiler, Andrew Packard, and Pascal Gahinet. An Introduction to Disk Margins [Lecture Notes]. *IEEE Control Systems*, (5):78–95, Oct. 2020. doi: 10.1109/mcs.2020.3005277.

[18] Tom Berger, Christina Ivler, Marcos Berrios, Mark Tischler, and David Miller. Disturbance Rejection Handling Qualities Criteria for Rotorcraft. 2016. doi: 10.4050/F-0072-2016-11452.